ELSEVIER

Journal of Molecular Catalysis A: Chemical 105 (1996) 193–201

JOURNAL OF MOLECULAR CATALYSIS A: CHEMICAL

A comparison of electrocatalytic ability of various mediators adsorbed onto paraffin impregnated graphite electrodes for oxidation of reduced nicotinamide coenzymes

Qi-Jin Chi, Shao-Jun Dong *

Laboratory of Electroanalytical Chemistry, Changchun Institute of Applied Chemistry, Chinese Academy of Sciences, Changchun, Jilin, 130022, P.R. China

Received 15 February 1995; accepted 5 May 1995

Abstract

Twelve mediators have been modified by adsorption onto the paraffin impregnated graphite electrodes (IGE). The resulting electrodes exhibit electrocatalytic activity of different degrees towards oxidation of 1,4-dihydronicotinamide adenine dinucleotide (NADH). The electrocatalytic ability of the chemically modified electrode (CME) depends mainly on the formal potential and molecular structure of mediator. The formation of the charge transfer complex between NADH and adsorbed mediator has been demonstrated by the experiments using a rotating disk electrode. An electrocatalytic scheme obeying Michaelis–Menten kinetics has been confirmed, and some kinetic parameters were estimated. The solution pH influences markedly the electrocatalytic activity of the modified electrode. Various possible reasons are discussed.

Keywords: Electrocatalysis; Graphite; Mediators; Nicotinamide coenzymes; Oxidation; Paraffin

1. Introduction

Many dehydrogenases use the coenzyme – nicotinamide adenine dinucleotide (NAD^+) producing the reduced form NADH. Therefore, the electrochemical oxidation of NADH continues to receive considerable attention due to an appeal for developing amperometric biosensors used in the determination of substrates. Unfortunately the direct oxidation of NADH at many bare electrodes is complicated and requires a large overvoltage [1–5], which results in the interference from more easily oxidizable species for the amperometric NADH detection in serum samples. Moreover the adsorbed molecules of NAD^+ will cause electrode fouling at NADH concentration above 0.1 $mmol \cdot dm^{-3}$ [6]. The electrocatalytic oxidation of NADH is an effective way for avoiding these problems. The oxidation of NADH has been achieved at many chemically modified electrodes (CMEs) at much lower voltages than at bare electrodes [7–25]. Different compounds such as quinones [11–14], alkyphenezinium [15] and phenoxazine [16–21] and phenothiazine [22–24] derivatives have been tried as mediators. However, only a restricted number of organic quinoid redox compounds seem to be able to mediate the electron transfer with electrodes [25]. The application of alkylphenazinium ions as the

* Corresponding author. Phone: (+86-431)682801, Fax: (+86-431)685653.

SSDI 1381-1169(95)00092-5

mediators is limited, due to their sensitivity to light [15]. In contrast, the phenoxazine and phenothiazine derivatives incorporating a charged *p*-phenylenediamine functionality are particularly appealing for the following reasons [26]: (a) NADH can be rapidly oxidized at these CMEs. (b) NADH oxidation does not cause electrode fouling [27], which is contrary to the bare electrodes [28] and the CMEs with other mediators [10,11]; and (c) the mediating properties seem to be selective for NADH, rather than electrodes incorporating other mediators [11,29]. In addition oxidation of NADH on the electrodes made of conducting organic salt NMP^+ $TCNQ^-$ has been reported by Albery and Bartlett [30]. They found that the electrodes readily oxidized NADH without deterioration for several days and were stable between −0.1 and 0.3 V (vs. SCE). Moreover the rate of oxidation was independent of electrode potential in this region. Electrocatalytic oxidation of NADH at the conducting polymer (poly(3-methylthiophene)) has been achieved recently [31]. The overvoltage for oxidation of NADH was decreased by 200 to 800 mV compared to platinum and glassy carbon electrodes, depending on the electrolyte and preparation procedures of the polymer film. Gorton et al. have summarized in detail electrocatalytic oxidation of nicotinamide adenine dinucleotide cofactor at the chemically modified electrodes [32]. These CMEs have been extensively used in the fabrication of the dehydrogenase-based biosensors [33–37].

In this paper, we have systematically compared electrocatalytic ability of twelve mediators adsorbed on the IGEs towards oxidation of NADH, and confirmed that the electrocatalytic activity mainly depends on the formal potential and the molecular structure of mediators.

2. Experimental

NADH was obtained from Shanghai Institute of Biochemistry, Chinese Academy of Sciences. The exact concentration of the NADH solutions was calculated from spectrophotometric assays at 340 nm using a molar absorptivity of 6220 $dm^3 \cdot mol^{-1} \cdot cm^{-1}$ [22]. Meldola Blue, Nile Blue A and Variamine Blue B were purchased from Chroma Chem. Co. and of analytical grade. Phenazine methosulfate was obtained from Fluka (>99%). Other mediators were of analytical grade and obtained from the Second Factory of Shanghai Reagent (China). Other reagents used were of analytical grade. All solutions were prepared with double-distilled deionized water. The supporting electrolyte solutions contained 0.1 $mol \cdot dm^{-3}$ phosphate buffer ($KH_2PO_4 + K_2HPO_4$) at pH 4.3–8.0. Other pH value solutions were obtained by adding either 0.1 $mol \cdot dm^{-3}$ HCl or 0.1 $mol \cdot dm^{-3}$ NaOH solution to phosphate buffer. The twelve mediators are abbreviated as follows: Methylene Blue (MB), Toluidine Blue (TB), Brilliant Cresyl Blue (BCB), Methylene Green (MG), Nile Blue A (NBA), Variamine Blue B (VBB), Meldola Blue (MdB), Azure I (AI), Azure II (AII), phenazine methosulfate (PMS), riboflavin (RF) and phenothiazine (PT).

Electrochemical experiments were carried out on an FDH 3204 potentiostat (Shanghai, China) associated with a Gould Series-60000 *X–Y* recorder (Shenyang, China). A three-electrode system was employed with an Ag/AgCl (saturated KCl) as reference electrode and a platinum plate as auxiliary electrode. Rotating disk electrode experiments were performed on a Model ATA-1A rotator (Shanghai University of Technology, China) and made a slow positive scan ($10\ mV \cdot s^{-1}$). All buffer solutions were deoxygenated for over 30 min before electrochemical experiments. All experiments were carried out at room temperature ($20 \pm 2°C$).

A spectroscopic graphite rod was cut into length of 0.8 cm, extracted in anhydrous methanol for 24 h to remove organic contaminants, dried and placed in melted paraffin to be impregnated with it for 30 min. The resulting rod was tightly sealed in shrinkable Teflon tube to form a disc electrode. Prior to use, it was polished with fine wet emery paper (grain size 700) and ultrasonicated in water

bath to remove any loose particles. The effective surface area (A) of the IGE was determined from electrochemical measurements of potassium ferricyanide to be 0.25 cm^2. The CMEs were prepared by immersing the bare electrodes in the solution containing 1 $mmol \cdot dm^{-3}$ mediator for a given time. The amount of mediator attached to the electrode surface was estimated from the average charge consumed by integrating area of cathodic and anodic peaks according to $Q = nFA\Gamma$.

3. Results and discussion

3.1. A comparison of electrocatalytic ability

Fig. 1 shows the typical irreversible oxidation of NADH at the bare IGE. The anodic peak is observed at +0.65 V with an overvoltage of ca. 1.2 V (for NAD^+/NADH, $E^{\circ\prime} = -0.56$ V vs. SCE or $= -0.52$ V vs. Ag/AgCl (saturated KCl) at pH 7.0 [2,3]). Therefore, a large overvoltage is required for direct oxidation of NADH at the bare IGE.

The molecular structure of eleven mediators is shown in Fig. 2. They are PT, four phenothiazine derivatives, three phenoxazine derivatives, RF, PMS and VBB. AII is not shown here, because it is a mixture of AI and MB in equal amounts. These

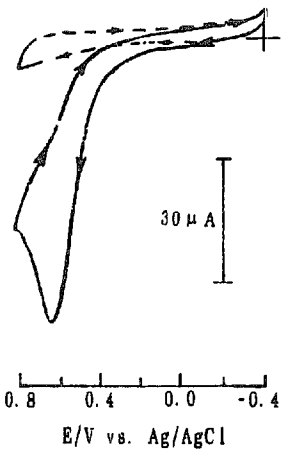

Fig. 1. Cyclic voltammograms of NADH oxidation at the bare graphite electrode in 0.1 $mol \cdot dm^{-3}$ phosphate buffer (pH 7.0). NADH concentration: 0 (dashed line) and 2.5 $mmol \cdot dm^{-3}$ (solid line); scan rate, 20 $mV \cdot s^{-1}$.

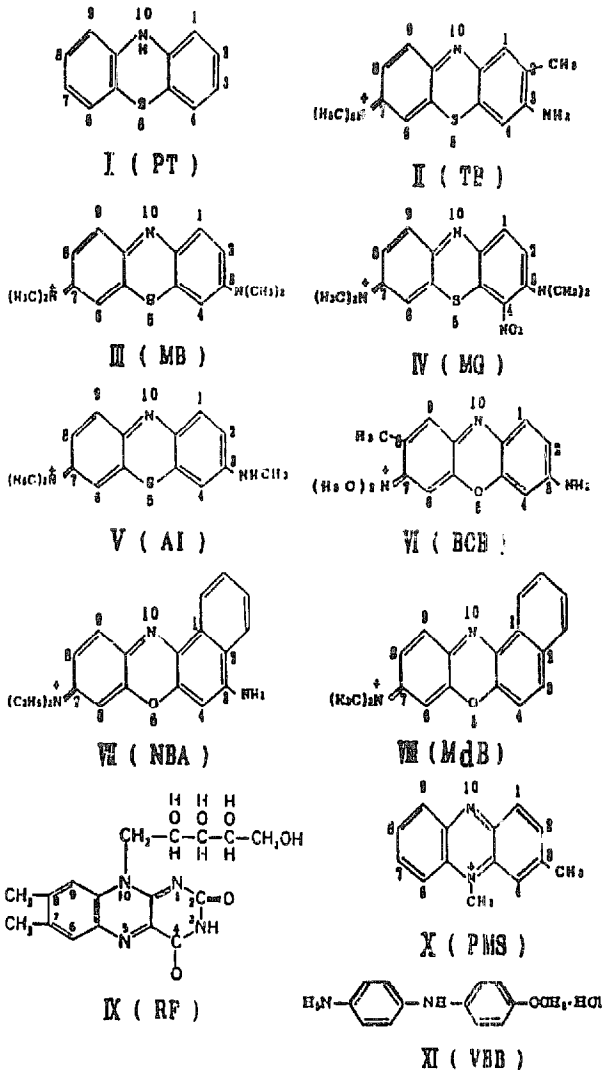

Fig. 2. The structural formulae of various mediators used in the present paper.

mediators can be irreversibly adsorbed on to the IGE surfaces to yield the stable CMEs. In order to avoid becoming involved in a much more complicated picture in the evaluation of rate constant between NADH and adsorbed mediator, it is especially important to control a monolayer or less of the mediator on the electrode surface. Therefore, the surface coverages of the adsorbed mediators were controlled by limiting the adsorption time and are about $1.5 \pm 0.2 \times 10^{-10}$ $mol \cdot cm^{-2}$ in the present experiments. Such surface coverages can ensure that the adsorbed mediators is approximately a monolayer.

Fig. 3 shows the oxidation of NADH at various mediator modified electrodes. The effective elec-

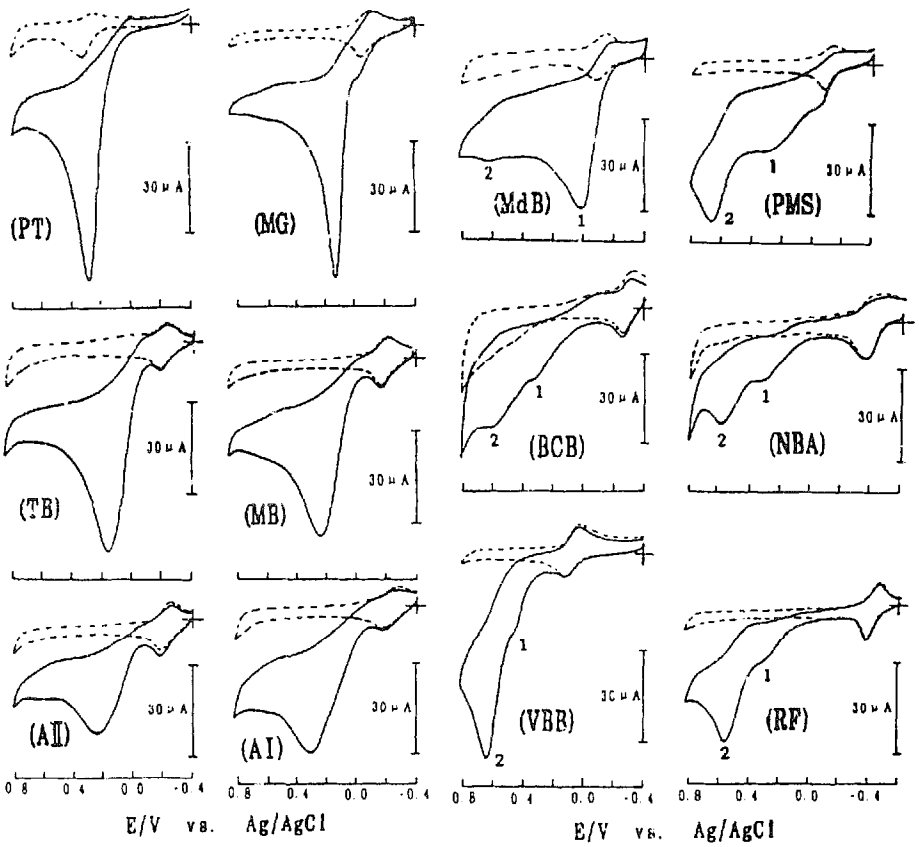

Fig. 3. Cyclic voltammograms of NADH oxidation at twelve different modified electrodes in 0.1 mol·dm^{-3} phosphate buffer (pH 7.0). NADH concentration: 0 (broken lines) and 2.5 mmol·dm^{-3} (solid lines); scan rate, 20 mV·s^{-1}.

trocatalysis is obtained, when PT, MG, TB, MB, AII, AI and MdB are used as mediators. At other modified electrodes, the oxidation of NADH seems to be more complicated, two anodic peaks are observed (Fig. 3). The potential of peak 2 is almost consistent with that of NADH oxidation at the bare graphite electrode, moreover its limiting current depends linearly on the square root of the rotating rate and Koutecky–Levich plot pass through the origin of coordinate. The results show that peak 2 is a non-catalytic peak and should be due to direct oxidation of NADH molecules passing through the modifier film and reaching the IGE surface. In contrast, peak 1 results from the electrocatalytic oxidation of NADH. Consequently the two oxidation processes for NADH at these CMEs really coexist, moreover they compete with each other. In these two processes of electrode reactions (electrocatalysis and non-electrocatalysis), which one predominates depends on the electrocatalytic ability of mediator adsorbed on the IGE surface. As shown in Fig. 3, when the CMEs possess excellent electrocatalytic ability, NADH is completely oxidized through electrocatalysis at these CMEs. At the other five CMEs the direct oxidation of NADH predominates over electrocatalysis, because the current of peak 2 is much larger than that of peak 1. This demonstrates that BCB, NBA, RF, PMS and VBB are poor catalysts for the NADH oxidation.

The parameters of the electrocatalytic oxidation of NADH at various CMEs obtained under the same experimental conditions are summarized in Table 1. The order of the catalytic rate is as follows: MdB > MG > TB > MB > PT > AII > AI > PMS > RF > NBA > BCB > VBB, which are basically consistent with that of the decrease degrees of overvoltage (except for PT). Obviously the electrocatalytic activity of the CMEs depends on the formal potential of the mediator, the more effective electrocatalysis can be obtained at the electrodes modified by the

Table 1
Parameters of the electrocatalytic oxidation of NADH at the graphite electrode modified by various mediators in 0.1 mol·dm^{-3} phosphate buffer (pH 7.0)

Mediators	$E^{\circ\prime}$/V	$E_{p,cat}$/V	E/mV	$i_{p,cat}$/μA [b]	10^{-4}/(M·s)$^{-1}$ [c]
MdB	−0.120	0.00	650	46	3.86
MG	−0.115	0.12	530	64	1.87
TB	−0.210	0.16	490	62	1.01
MB	−0.210	0.24	410	52	0.80
AII	−0.220	0.25	400	30	0.64
AI	−0.225	0.30	350	41	0.63
PT	+0.280	0.28	370	63	0.71
PMS	−0.110	0.30	350	20	0.42
RF	−0.430	0.32	330	13	0.083
NBA	−0.405	0.32	330	22	0.034
BCB	−0.280	0.35	300	15	0.024
VBB	+0.095	0.45	200	17	0.009

[a] $E^{\circ\prime}$, $E_{p,cat}$, E and $i_{p,cat}$ represent formal potential of mediator, catalytic peak potential, decrease in overvoltage and catalytic peak current, respectively.
[b] Obtained at 2.5 mmol·dm^{-3} NADH and 20 mV·s^{-1}.
[c] Obtained at 0.5 mmol·dm^{-3} NADH and pH 6.0.

mediators with formal potential of between −0.1 and −0.25 V at pH 7.0. On the other hand, the electrocatalytic ability of the CMEs is related to the mediator structure. The slight difference in structure of mediator results in a marked difference of the electrocatalytic activity, which is obviously observed between MG and MB and between MdB and NBA. Such a structural-dependent profile is possibly associated with the mechanism of the electrocatalytic reaction, so it will be further discussed in the following section. In addition, a mediator with a high catalytic reaction rate is usually expected to have a catalytic peak potential very close to the anodic peak potential obtained in the absence of NADH and also a high catalytic current. However, in the present experiments some unexpected results are found. As shown in Fig. 3 and Table 1, the PT/IGE has a large catalytic current but a smaller reaction rate, the contrary situation is obtained from the MdB/IGE. The exact reason is not clear at the present time, probably these results are caused by the impurity of the commercial mediator used here, as was indicated in the literature [38].

3.2. Mechanism of the electrocatalytic reaction

The reaction mechanism between NADH and adsorbed organic dyes has been investigated in detail by Gorton et al [17–19,26] and found to be similar to the Michaelis–Menten kinetics. Here the MG/IGE as an example was used in the study of the electrocatalytic mechanism in the present experiments. Fig. 4 shows Levich plots obtained at the MG/IGE at various NADH concentrations. The limiting current of NADH oxidation increases with increasing rate of rotation (ω), an evident deviation from the straight line is observed at higher ω. The corresponding Koutecky–Levich plots all give straight lines and the intercepts of all straight lines deviate from origin, as shown in Fig. 5. Such behaviour is expected for a reaction with a chemical rate-limiting step [39]. It is noted that the intercepts of the curves shown in Fig. 5 change with NADH concentrations, this indicates that the electrocatalytic reaction rate depends on NADH concentration. The result implies that the

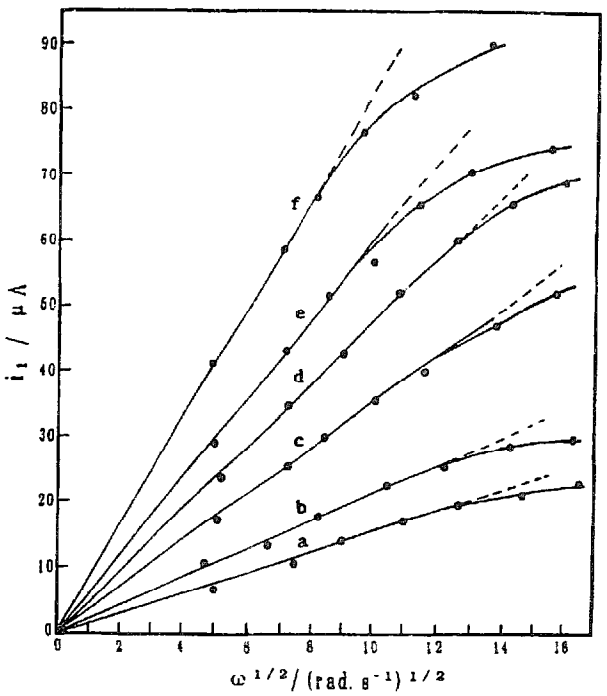

Fig. 4. Levich plots obtained at the MG/IGE at various NADH concentrations (mmol·dm^{-3}): 0.125 (a), 0.250 (b), 0.375 (c), 0.500 (d), 0.625 (e) and 1.000 (f). In 0.1 M phosphate buffer (pH 6.0); surface coverage, $(1.5 \pm 0.2) \times 10^{-10}$ mol·cm^{-2}; scan rate, 10 mV·s^{-1}; line scans were carried out from −0.4 to +0.6 V (vs. Ag/AgCl).

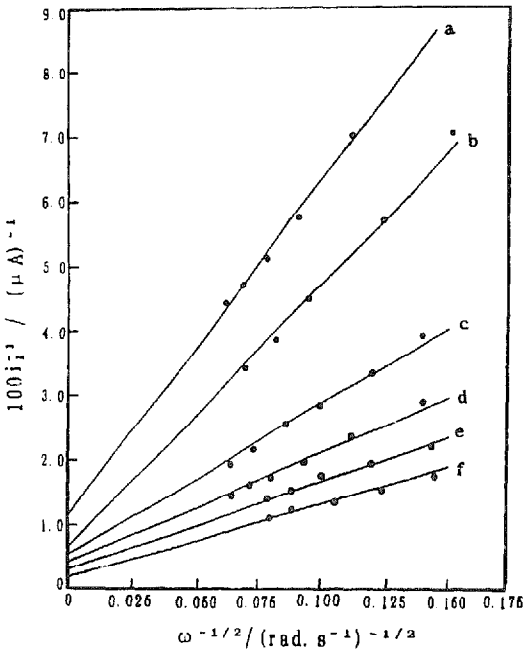

Fig. 5. Koutecky–Levich plots of the same data shown in Fig. 4.

electrocatalytic mechanism possibly obeys Michaelis–Menten kinetics, so the reaction scheme similar to the Michaelis–Menten expression [40] is assumed as follows:

$$\mathrm{NADH} + \mathrm{MG}^{+} \underset{k_{-1}}{\overset{k_{+1}}{\rightleftharpoons}} [\mathrm{NADH}\cdot\mathrm{MG}^{+}] \xrightarrow{k_{+2}} \mathrm{NAD}^{+} + \mathrm{MGH} \quad (1)$$

According to Michaelis–Menten method, combination k_{+1}, k_{-1} and k_{+2} to give

$$K_{\mathrm{M}} = (k_{-1} + k_{+2})/k_{+1} \quad (2)$$

Such, the rate constant of the electrocatalytic reaction (k) can be expressed as [17]

$$k = k_{+2}/(K_{\mathrm{M}} + C^{*}) \quad (3)$$

Inversion of eqn(3) gives

$$1/k = K_{\mathrm{M}}/k_{+2} + C^{*}/k_{+2} \quad (4)$$

where C^{*} is the bulk concentration of NADH.

If the assumption of the formation for a charge-transfer complex (shown in Eq. (1)) is true, the plot of $1/k$ against C^{*} will give a straight line. Good agreement is obtained between experimental results and theoretical prediction, as shown in Fig. 6. The two constants k_{+2} and K_{M} were calculated as 26 s^{-1} and 0.88 mmol·dm^{-3}, respectively, from the slope and intercept of the plot shown in Fig. 6. However, the reaction scheme described in Eq. (1) cannot explain completely the dependence of the electrocatalytic activity on the mediator structure and the solution pH values. This shows that the real reaction scheme must be more complicated than that shown in Eq. (1).

As illustrated in Table 1, the catalytic reaction rate constants at the MG/IGE and MdB/IGE are, respectively, over 2 times and 100 times than those at the MB/IGE and the NBA/IGE. The decreases in overvoltage are 650 mV for MdB/IGE, 330 mV for NBA/IGE, 530 mV for MG/IGE and 410 mV for MB/IGE, respectively. MG contains a nitro-group at the 4-position, whereas MB does not (Fig. 2, III and IV). Similarly NBA possesses an amino-group at the 3-position, whereas MdB does not (Fig. 2, VII and VIII). As is known, the nitro-group and amino-group are strong electron acceptor group and donor group respectively. In order to understand better the marked difference of electrocatalytic ability resulting from the slight difference of mediator structure, the electrocatalytic reaction scheme is further assumed as follows [18]:

$$\mathrm{NADH} + \mathrm{M} \underset{k_{-1}}{\overset{k_{+1}}{\rightleftharpoons}} \underset{\mathrm{I}}{[\mathrm{NADH}\cdot\mathrm{M}]} \rightleftharpoons \underset{\mathrm{II}}{[\mathrm{NADH}^{+\cdot}\cdot\mathrm{M}^{-\cdot}]} \quad (5)$$

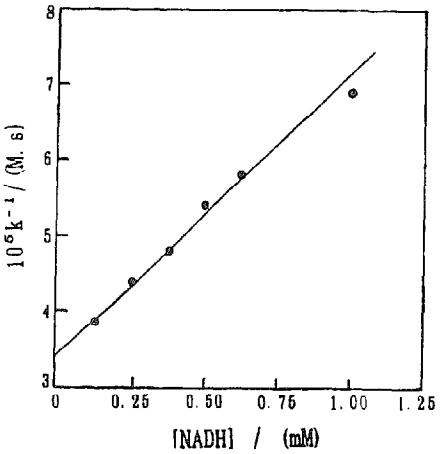

Fig. 6. The dependence of the reciprocal value of the electrocatalytic rate constant on the concentration of NADH. The data obtained from Fig. 5.

$$[NADH^{+\cdot}\cdot M^{-\cdot}] + H_2O \rightarrow NAD^{\cdot} + M^{-\cdot} + H_3O^{+} \quad (6)$$

$$M^{-\cdot} + H_3O^{+} \rightarrow MH^{\cdot} + H_2O \quad (7)$$

$$NADH + MH^{\cdot} \rightarrow NAD^{\cdot} + MH_2 \quad (8)$$

$$NAD^{\cdot} \rightarrow NAD^{+} + e \quad (9)$$

$$MH_2 \rightarrow M + 2H^{+} + 2e \quad (10)$$

$$2NADH \rightarrow NAD^{+} + 2H^{+} + 3e + NAD \quad (11)$$

where M represents the oxidized mediator.

At first a complex (I) forms, and then the charge exchange takes place between NADH and M to generate complex II. In the complex (II), the mediator possesses part negative charge. When the acceptor group exists in the mediator molecule, it will enhance the stability of the complex (II). In contrast, the donor group will decrease the stability of the complex (II). This is possibly the main reason why MG and MdB are more effective catalysts, respectively, compared to MB and NBA.

3.3. The effect of the solution pH

Fig. 7 shows the cyclic voltammograms of NADH oxidation at the MdB/IGE in the different pH solutions. Only an anodic peak is observed at pH below 7.0 (Fig. 7A–C), whereas two anodic peaks occur at pH above 7.0 (Fig. 7D–G). As described above, peaks 1 and 2 correspond to the electrocatalytic and direct oxidation of NADH, respectively. The current of peak 1 increases with pH up to 6.0, and then decreases drastically above pH 6.0 (Fig. 8a). In contrast, the current of peak 2 gradually increases with increasing pH value (Fig. 8b). Obviously the electrocatalysis is more effective with NADH oxidized completely through the electrocatalytic pathway in slight acid media. However, it is noted that the catalytic current also decreases markedly in the solutions below pH 6.0, moreover almost no catalytic current can be measured at pH below 2.0. This is mainly caused by the decomposition of NADH which results in losing a substantial amount of the initial concentration of NADH at lower pHs. As discussed in the previous report, NADH is stable in base but labile in acid, moreover its decomposition is especially rapid in phosphate buffer. The half-life of NADH below pH 4 can be approxi-

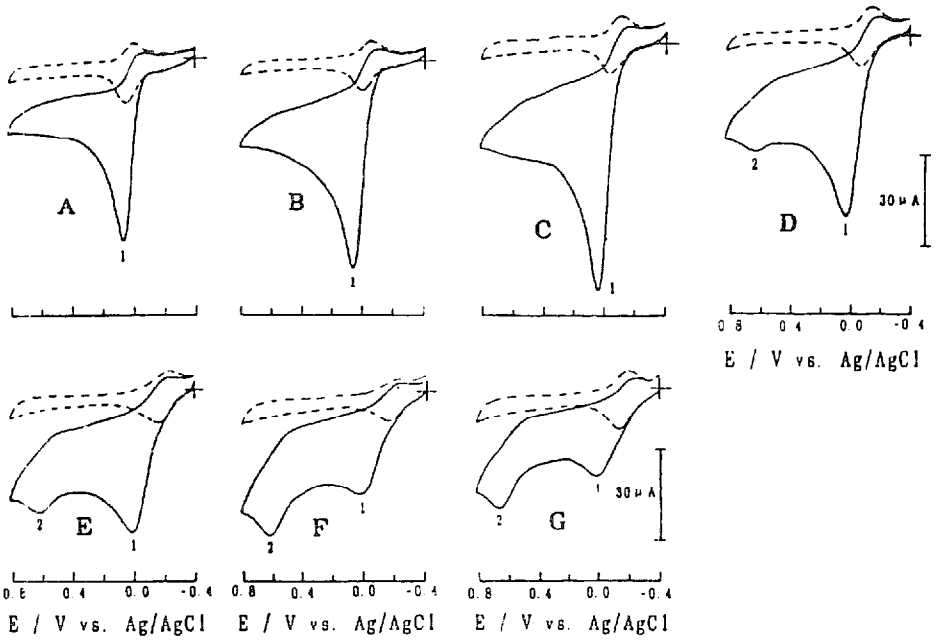

Fig. 7. Cyclic voltammograms of NADH oxidation at the MdB/IGE in different pH solutions. pH values: 3.8 (A), 4.8 (B), 6.0 (C), 7.0 (D), 8.0 (E), 9.0 (F) and 10.0 (G). NADH concentrations: 0 (broken lines) and 2.5 mmol·dm^{-3} (solid lines); scan rate, 20 mV·s^{-1}.

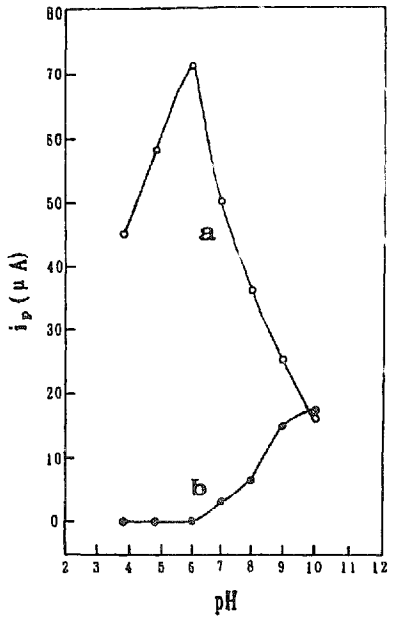

Fig. 8. Variation of the peak currents with solution pH values. The data from Fig. 7, curve a and b represent peak 1 and 2 shown in Fig. 7, respectively.

mately estimated as 1000 s [41]. Such a decomposition rate makes it difficult to avoid the decrease in the NADH bulk concentration, when the experiments are performed at the lower pHs. On the other hand, the direct oxidation of NADH gradually predominates with increasing pH, at pH above 7.0. There are several possible explanations for such pH-dependent behaviour. Firstly, the electrocatalytic process involves the protons as described in Eqs. (6–10). The second possibility is that the orientation of the adsorbed mediator on the electrode surface changes with pH, which will affect electrocatalytic activity if the catalytic sites of the electrode surface become inaccessible with reorientation. For adsorbed Nile Blue A, this phenomenon has been demonstrated by Raman spectra experiments [26]. The third one is that adsorbed mediator has poor stability in alkaline solutions compared with that in acid media, which is what was observed in the present experiments. However, the real reason is possibly more complicated and requires further study.

4. Conclusion

The CMEs have been prepared by adsorption of various mediators onto the paraffin impregnated graphite electrodes and used in the electrocatalytic oxidation of NADH. Two oxidation processes of NADH at these CMEs are observed, moreover they compete with each other depending on the electrocatalytic ability of the CMEs. The electrocatalytic activity of the CMEs associates with the formal potential and molecular structure of the mediator, and is also affected by solution pH. The electrocatalytic reaction scheme is assumed and used to explain experimental results.

Acknowledgements

The support of the National Natural Science Foundation of China is gratefully appreciated.

References

[1] W.J. Blaedel and R.A. Jenkins, Anal. Chem., 47 (1975) 1337.
[2] P.J. Elving, C.O. Schmakel and K.S.V. Santhanam, Crit. Rev. Anal. Chem., 6 (1976) 1.
[3] J. Moirous and P.J. Elving, Anal. Chem., 50 (1978) 1056.
[4] H. Jaegfeldt, J. Electroanal. Chem., 110 (1980) 295.
[5] P.J. Elving, W.T. Rersnahan, J. Moirous and Z. Samec, Bioelectrochem. Bioenerg., 9 (1982) 365.
[6] J. Moirous and P.J. Elving, J. Electroanal. Chem., 102 (1979) 93.
[7] C. Degrad and L.L. Miller, J. Am. Chem. Soc., 102 (1980) 5728.
[8] M. Fukui, A. Kitani, C. Degrand and L.L. Miller, J. Am. Chem. Soc., 104 (1982) 28.
[9] H. Huck and H.L. Schmit, Angew. Chem., 50 (1981) 421.
[10] H. Jaefeldt, T. Kuwana and G. Johansson, J. Am. Chem. Soc., 105 (1983) 1805.
[11] D.C.S. Tse and T. Kuwana, Anal. Chem., 50 (1978) 1315.
[12] H. Jaefeldt, A.B.C. Torstensson, L. Gorton and G. Johansson, Anal. Chem., 53 (1981) 1979.
[13] K. Ravichandran and P.P. Baldwin, J. Electroanal. Chem., 126 (1981) 293.
[14] C. Ueda; D.C.S. Tse and T. Kuwana, Anal. Chem., 54 (1982) 850.
[15] A. Torstensson and L. Gorton, J. Electroanal. Chem., 130 (1981) 199.
[16] H. Huck, Fresenius' Anal. Chem., 313 (1982) 548.
[17] L. Gorton; A. Torstensson; H. Jaefeldt and J. Johansson, J. Electroanal. Chem., 161 (1984) 103.
[18] L. Gorton, G. Johansson and A. Torstensson, J. Electroanal. Chem., 196 (1985) 81.
[19] L. Gorton, J. Chem. Soc., Faraday. Trans. 1, 82 (1986) 1245.
[20] H. Huck, A. Schelter-Graf and H.L. Schmidt, Bioelectrochem. Bioenerg., 13 (1984) 199.

[21] B. Persson and L. Gorton, J. Electroanal. Chem., 292 (1990) 115.
[22] B. Persson, J. Electroanal. Chem., 287 (1990) 61.
[23] K. Hajizadeh, H.T. Tang, H.B. Halsall and W.R. Heineman, Anal. Lett., 24 (1991) 1453.
[24] J. Kulys, Electroanalysis, 5 (1993) 201.
[25] A. Kitani, Y.H. So and L.L. Miller, J. Am. Chem. Soc., 103 (1981) 7636.
[26] F. Ni, H. Feng, L. Gorton and T.M. Cotton, Langmuir, 6 (1990) 66.
[27] R. Appelqvist, G. Marko-Varge, L. Gorton, A. Torstensson and G. Johansson, Anal. Chim. Acta, 169 (1985) 237.
[28] Z. Samec and P.J. Elving, J. Electroanal. Chem., 144 (1983) 217.
[29] K. Mckenna, S.E. Boyette and A. Brajter-Toth, Anal. Chim. Acta, 206 (1988) 75.
[30] W.J. Albery and P.N. Bartlett, J. Chem. Soc., Chem. Commun., (1984) 234.
[31] N.F. Atta, A. Galal, A.E. Karagozler, H. Zimmer, J.F. Rubinson and H.B. Mark, Jr., J. Chem. Soc., Chem. Commun., (1990) 1347.
[32] L. Gorton, B. Persson, P.D. Hale, L.I. Boguslavsky, H.I. Karan, H.S. Lee, T. Skotheim, H.L. Lan, Y. Okamoto, P.G. Edelman and J. Wang (Eds.) Biosensors and Chemical Sensors, ACS Symp. Ser., 487 (1992) 56–83.
[33] G. Bremle, B. Persson and L. Gorton, Electroanalysis, 3 (1991) 77.
[34] L. Gorton, G. Bremle, E. Csoregi, G. Jonsson-Petterson and B. Persson, Anal. Chim. Acta, 249 (1991) 43.
[35] B. Persson, H.L. Lan, L. Gorton, Y. Okamoto, P.D. Hale, L.I. Boguslavsky and T. Skotheim, Biosensors and Bioelectronics, 8 (1993) 81.
[36] E. Dominguez, H.L. Lan, Y. Okamoto, P.D. Hale, T.A. Skotheim and L. Gorton, Biosensors and Bioelectronics, 8 (1993) 167.
[37] E. Dominguez, H.L. Lan, Y. Okamoto, P.D. Hale, T.A. Skotheim, L. Gorton and B. Hahn-Hagerdal, Biosensors and Bioelectronics, 8 (1993) 229.
[38] J. Kulys, G. Gleixner, W. Schuhmann and H.L. Schmidt, Electroanalysis, 5 (1993) 201.
[39] R.D. Rocklin and R.W. Murray, J. Phys. Chem., 85 (1981) 2104.
[40] L. Michaelis and M. Menten, Biochem. Z., 49 (1913) 333.
[41] F. Ni, L. Thomas and T.M. Cotton, Anal. Chem., 61 (1989) 888.